5375

Diffusion restriction along fibres: How coherent is the corpus callosum?

Jeroen Mollink[1], Michiel Kleinnijenhuis[1], Stamatios N Sotiropoulos[1], Olaf Ansorge[2], Saad Jbabdi[1], and Karla L Miller[1]

[1]*Nuffield Department of Clinical Neurosciences, FMRIB centre, University of Oxford, Oxford, Oxfordshire, United Kingdom,* [2]*Nuffield Department of Clinical Neurosciences, Neuropathology, University of Oxford, Oxford, Oxfordshire, United Kingdom*

PURPOSE. Diffusion weighted imaging aims to unravel the microstructural properties of white matter in the brain by detecting alterations to diffusive motion along different orientations. Increasingly sophisticated biophysical models are used to estimate properties like fibre orientation dispersion in addition to mean orientation. Most models assume an explicit or implicit assumption that water is able to diffuse freely along the primary fibre orientation. However, microstructural analysis with histology and electron microscopy in both rodent and human brains demonstrated a considerable amount of dispersion even in the corpus callosum [1,2,3], which is often used as a test-bed for diffusion models [4] based on its assumed extreme fibre coherence. The present study aims to investigate the coherence of fibre orientations at multiple scales in the human corpus callosum using two modalities: diffusion-time (Δ) MRI measurements and direct estimation of fibre orientation from optical microscopy (polarized light imaging, PLI). A secondary aim of this work is to demonstrate the potential for using PLI-MRI comparisons in the same tissue sample to inform biophysical modeling aimed at in vivo diffusion MRI.

METHODS. **Diffusion MRI:** A 5 mm coronal slab was excised from a postmortem formalin fixed brain at the level of the anterior commissure, including the medial corpus callosum and the gyri cinguli. Prior to imaging, the specimen was soaked in PBS for 72 hours. It was scanned in a container filled with Fluorinert (3M). Postmortem diffusion imaging was performed on a 9.4 T Varian MRI scanner with a 25 mm quadrature birdcage coil (Rapid Biomedical). A diffusion weighted spin echo (DW-SE) sequence was used to acquire the diffusion data at 0.4 mm isotropic resolution, with b=[2500, 5000] s/mm^2, a TR/TE of 2.4s/29ms and 240 diffusion gradient directions (δ=6ms, Δ=16ms). Diffusion-weighted STEAM data were acquired with diffusion gradients (δ=2.22 ms) applied in 30 directions distributed over a hemisphere for 9 diffusion times Δ = [35 70 100 150 200 250 300 350 400] ms with a fixed q-value (with removal of crusher gradients to avoid b-value contamination). For each diffusion time, a non-diffusion weighted image was acquired. Imaging parameters: 10 slices with 0.4 mm isotropic voxels, TE=16ms, TR=2.4-4.1 s (minimized for each diffusion time). The apparent diffusion coefficient (ADC) was calculated in three ROIs for perpendicular and parallel diffusion (i.e. with respect to the principal diffusion direction computed from a diffusion tensor fit to the DW-SE data) at each diffusion time. The ROIs were defined in the corpus callosum, two lateral parts (left and right, CC_L and CC_R, respectively) and one medial part (CC_M). To estimate within-voxel orientation dispersion from the DW-SE data, the ball and racket model was fitted [5] **PLI:** Following MRI, the sample was cryoprotected, frozen at -80 °C and cut in 60 µm sections. The unstained sections were mounted on glass slides and coverslipped using a PVP mounting medium. PLI was performed with a polarizing microscope (Leica DM4000B, upgraded with a circular polarizer and a rotatable analyzer) and fibre orientation maps (FOM) were computed according to the methods described by Axer et al [6]. In-plane fibre dispersion was estimated by fitting the fibre orientation distribution (FOD) with a von Mises distribution within an n x n neighborhood, with n=[80, 200, 400, 600, 1000, 2000] µm for two tissue sections. The concentration parameter (κ) of the orientation distribution is inversely proportional to the dispersion (1/κ). Dispersion analyses were performed for three ROI's defined in a similar manner as described for ADC analysis.

RESULTS/DISCUSSION. Figure 1 shows the in-plane fibre orientation maps for both DW-SE and PLI, demonstrating excellent correspondence of the macroscopic detail available in the diffusion MRI data. However, the PLI data exhibits considerable heterogeneity at the mesoscopic scale, in particular with clear incoherence of fibres at the midline (CC_M) and extreme lateral aspects of the corpus callosum (near the centrum semiovale). Within-voxel dispersion based on the DW-SE data shows higher dispersion in CC_M than at lateral regions of the corpus callosum (Fig. 2A). For the very long diffusion times employed, ADC behaves as if hindered both across and along the axonal orientation (i.e. ADC decreases with diffusion time, Fig. 2B). This ADC dependence was found to be remarkably similar in the three ROIs, despite the different appearance of the CC_M in both within-voxel dispersion (Fig. 2A) and PLI data. Orientation distributions were fitted to the PLI fibre orientation maps over a local neighborhood at various scales (Fig. 2C) and mean dispersion values were computed for these spatial scales (Fig. 2D). At coarse scales (i.e. n > 500 µm), the CC_M region experiences more fibre dispersion than the lateral regions of the corpus callosum, i.e CC_L and CC_R corresponding to the heterogeneity evident by eye in the PLI (Fig. 1B and 2C). However, the dispersion was similar across the corpus callosum at microscopic scales (i.e. n < 200 µm).

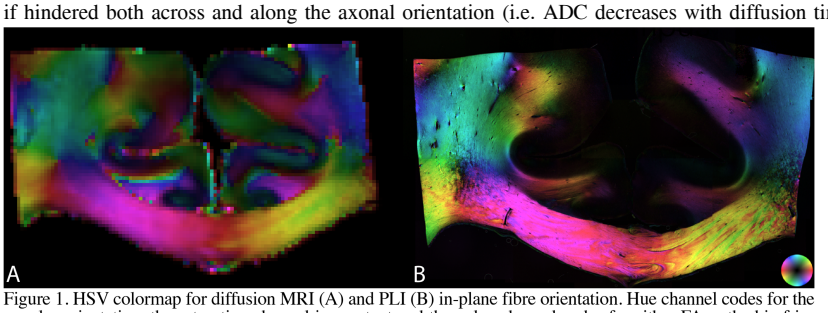

Figure 1. HSV colormap for diffusion MRI (A) and PLI (B) in-plane fibre orientation. Hue channel codes for the angular orientation, the saturation channel is constant and the value channel codes for either FA or the birefringence in diffusion MRI and PLI, respectively.

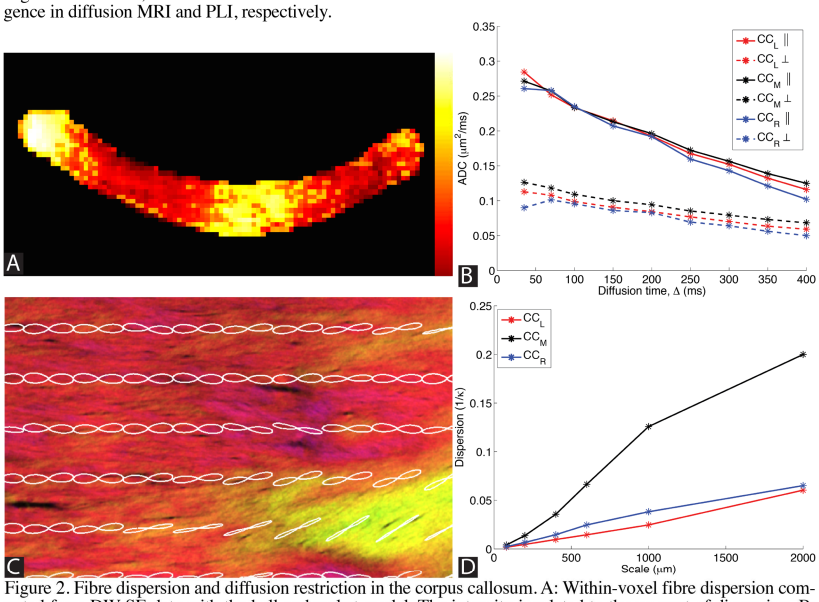

Figure 2. Fibre dispersion and diffusion restriction in the corpus callosum. A: Within-voxel fibre dispersion computed from DW-SE data with the ball and racket model. The intensity is related to the amount of dispersion. B: ADCs from DW-STEAM data at different diffusion times for diffusion parallel and perpendicular to the fibre orientation in the corpus callosum regions. C: PLI fibere orientation map (see Figure 1 for description) overlaid with fiber orientation distribution for a neighborhood size of 400x400 µm^2. D): PLI fiber dispersion accros corpus callosum regions at various spatial scales.

CONCLUSION. The fibre orientations found with diffusion imaging in the present study exhibit an excellent match with fibre orientations mapped with PLI at a macroscopic scale. Regarding the corpus callosum, a considerable amount of fibre dispersion was observed from the PLI data. This dispersion cannot be neglected and confirms that the hypothesis to consider the corpus callosum as a model for coherent fibre orientations may not always be appropriate. Furthermore, it was particularly striking that the dispersion estimated from diffusion data (i.e. DW-SE data) in the medial part of the corpus callosum was higher compared to more lateral regions, which was confirmed with PLI. This has important implications for the common strategy of selecting the midsagittal slice as a reference of coherent fibre orientation. However, hindered diffusion along axonal orientation (from DW-STEAM data) across the corpus callosum was observed to be homogeneous. The mesoscopic fibre dispersion would therefore be less likely to explain the diffusion restriction along fibres in the corpus callosum. Microstructural dispersion in the examined regions is similar and might be the source of the observed restriction, but will need future work, for example diffusion simulations before drawing conclusions.

REFERENCES. [1] Leergaard, TB, PLoS One (2010); [2] Mikula, S, Nature Methods(2012); [3] Budde, MD, Front. Integr. Neurosci. (2013); [4] Nilsson, M, MAGMA (2013); [5] Sotiropoulos, SN, NeuroImage (2012); [6] Axer, M, NeuroImage (2011).